J. Fluid Mech. (1998), vol. 365, pp. 1–22. Printed in the United Kingdom

Instability of convective cells and genesis of convective structures of different scale

By V. M. MALBACKOV

Computing Centre, Lavrentiev Prospect 6, Novosibirsk 630090, Russia

(Received 5 April 1994 and in revised form 29 April 1997)

The paper is devoted to an investigation of convective turbulence. A simplified approach is used for this purpose. It considers an isolated turbulent pulsation as the eigensolution to the corresponding equations of thermohydrodynamics. Turbulence is generated by nonlinear interaction of pulsations: not all interactions, but only the most probable of them are investigated. It is assumed that during convection these are interactions of cells located along the gravity vector, i.e. lying in a vertical line, and lateral interaction of the cells is ignored. This assumption allows one to consider the process of the evolution and interaction of cells as axially symmetric. It is also assumed that the vertical scales of convective cells are larger than their horizontal scales. Therefore, the Boussinesq equations simplified in accordance with the theory of vertical boundary layers can be used. The fact that buoyancy forces, in addition to diffusion, influence the increase of the vertical scales, serves as a basis for this assumption. These assumptions make it possible to obtain the analytical and numerical–analytical solutions, which qualitatively describe the evolution and interaction of convective cells of two essentially different scales: (i) centimetre-scale convective pulsations and (ii) thermals and convective clouds, and to reduce the problem to the solution of nonlinear equations (equations of the Burgers type). Two opposite tendencies are revealed, manifested in the interaction of convective cells. First, there is coagulation of cells and fine nonlinear effects associated with it, which are known from observations and supported by the theory. Secondly, there is destruction of a strong rising cell through its collision with a weak descending 'cold' cell. It is assumed that the destruction of cells corresponds to the absence of solutions, when some parameters reach their critical values. A numerical solution to a more accurate problem without simplifications of the vertical boundary layer serves as a basis for this hypothesis. It shows that at critical values of the parameters the process of 'wave turnover' begins. It is accompanied by entrainment of the motions of the cold surrounding air into a system of convection and fast dissipation of a cell. In the simplified model, this dissipation is considered to be instantaneous and is called destruction. When the cells are sufficiently strong vertically, weak random fluctuations in the fields of meteorological elements cause their destruction. These results make it possible to propose a hypothesis which relates the degree of instability of cells with the probability of their existence, and to construct functions of cell distributions.

1. Introduction

'Convection' is usually understood as processes associated with vertical thermal unstable stratification of a liquid or gas. Rayleigh (1916) made the first successful attempt to explain the mechanism of formation of ordered convective structures in a viscous liquid placed in a cavity between two plane horizontal plates (Benard cells). Later laboratory and theoretical investigation of various laminar, turbulent and transient regimes of Rayleigh–Bénard convection have become the main apparatus in the theory of heat mass transfer. There are numerous applications of this apparatus in engineering, in the theory of convection in the atmosphere, ocean, Earth's mantle, stars, in the problem of the location of sources of heat and cold, in problems of optimal heating or cooling of liquid and gaseous media, etc. A large number of publications in periodicals, regional, national and international conferences are devoted to these problems. Lectures by leading specialists in Brighton on August 14–18, 1994 give an idea of the most important investigations of heat transfer. There are many papers in which some types of turbulent regimes are simulated numerically (Davaile & Jampart 1993; Decker, Petch & Weber 1994; Glukhovskaya & Ordanovitch 1993; Jimenez *et al.* 1993; Clever & Busse 1994; Noto, Yamamoto & Nakajima 1994). These models are used to explain the complex mechanism of turbulence, to test the existing methods of parameterization of turbulence, and to develop new methods. It has been found that the K and $K - \varepsilon$ models cannot be used to explain many important details of the mechanism of developed convective turbulence (Kurbatskii 1988). More complex models, which are based on second- and third-order closure schemes, have been developed in (Andre 1976; Ebert, Shuman & Stul 1989; Lykossov 1995). Direct application of the theory of convection to the atmosphere, which uses the solution to the Boussinesq equations, is difficult, because atmospheric convective processes are always turbulent. Simulation of these processes is, as a rule, based on the fact that small centimetre scale turbulent pulsations form mesoscale convective structures, i.e. thermals and convective clouds. Simulation of mesoscale two-dimensional coherent structures in parameterized small-scale three-dimensional turbulence is investigated in Glukhovskaya & Ordanovitch (1993). Also, satellite photographs show that clouds are often clustered into large disordered and quasi-ordered structures of various configurations. In the construction of atmospheric models of large-scale convection, perturbations of the scale of thermals and convective clouds, as well as smaller perturbations, are considered as turbulence and taken into account parametrically. The form of cloud populations can be explained with the help of such models (Malkus & Veronis 1958; Veltichev & Geokhlanian 1974). An essential shortcoming of the Rayleigh–Bénard models is an artificially given solid upper boundary, which is absent from the atmosphere. Models of penetrative convection do not have this shortcoming. They consider convective processes within the framework of the LES (large-eddy simulation) approach, and they allow for decrease in the air density with height, and attenuation of motions due to stable stratification of the upper layer. Atmospheric perturbations smaller than several tens of metres are taken into account parametrically in the LES models. The LES models are usually used to simulate a large number of convective cells: they serve to test various parameterizations of atmospheric convection. There are also papers in which the LES models are used to investigate ensembles of thermals and convective clouds (Deardorff 1974; Kruger, McLean & Qiang Fu 1995; Moeng, Lenshow & Rendal 1995). One line of investigation is the development of simplified parameterization models of convection for models of general circulation of the atmosphere. Simplified models, which take into account transport of heat, moisture (Kuo 1965, 1974) and momentum (Arakawa & Schubert 1974; Tiedtke 1983, 1989) in convective cells, have been used most successfully for these purposes. In the present paper, an attempt is made to combine the advantages of the LES models and those of the simplified approach. As in the LES models, interactions of cells are taken into account in the present paper. This makes it possible to obtain cell distribution functions. The models of convective cells and the allowance for their interaction are, however, very simplified. Therefore, solutions can be obtained in the analytical form. This gives hope that the solutions can be used for parameterization of convection in models of large-scale atmospheric processes. This parameterization can turn out to be more accurate than that used at present, because it takes into account, to a first approximation, the space structure of convective cells and their interaction. Also, the methods used in the present paper and the results obtained, although they are qualitative in character, can be of interest for specialists in heat mass transfer in liquids and gases.

The paper is devoted to an investigation of convective turbulence. For this purpose, a simplified approach, which considers each turbulent pulsation as the eigensolution to the corresponding equations of thermohydrodynamics, and in which turbulence is generated by nonlinear interaction of pulsations is used (Goldshtik 1985): not all interactions, but only the most probable of them are investigated. It is assumed that during convection this is the interaction of cells located along the gravity vector, i.e. lying in a vertical line, and lateral interaction of cells is ignored. This assumption makes it possible to consider the process of evolution and interaction of cells as axially symmetric. In addition, it is assumed that the vertical scales of convective cells are larger than their horizontal scales, which allows one to use the Boussinesq equations simplified by the theory of vertical boundary layers in the investigation of convection. The fact that buoyancy forces, in addition to diffusion, affect the increase in vertical scales, is the basis of this assumption. It should be noted that such serious simplifying assumptions on the character of convection are not fulfilled in reality: they are introduced to obtain accurate solutions, investigate the evolution and interaction of convective cells and develop a hypothesis that allows one to go from the hydrodynamic model to a simplified statistical model. It is assumed that this model will qualitatively explain the sizes and lifetimes of micro- and mesoscale atmospheric convective cells, i.e. it will qualitatively explain the main statistical characteristics of atmospheric convection. Use of the hydrodynamic model even substantially simplified for justification of statistical characteristics of convection is a step forward in comparison to the traditional approach, which usually uses empirical models for this purpose.

2. Mathematical formulation of the problem

Let us consider the problem of the interaction of several convective cells initiated by thermal pulses given at the initial moment of time. The problem is solved under the following simplified assumptions: convection develops in the polytropic atmosphere, i.e. the temperature is a linear function of height; vertical scales of convective cells are larger than their horizontal scales and, therefore, the initial equations are derived from thermodynamic equations using the simplifications of the theory of vertical boundary layer (Gutman 1969) (see Appendix A); both convective cells and thermal pulses are axially symmetric and located on the vertical axis; coefficients of turbulent viscosity and heat conductivity are equal and do not depend on the coordinates and time.

After the simplifications of the convection theory and the theory of vertical boundary layers (see Appendix A), the thermohydrodynamic equations have the following form (Gutman 1969; Malbackov 1978):

$$\left.\begin{aligned} \frac{\partial w}{\partial t}+u\frac{\partial w}{\partial r}+w\frac{\partial w}{\partial z} &= \lambda\vartheta+\frac{v}{r}\frac{\partial}{\partial r}r\frac{\partial w}{\partial r}+v\frac{\partial^2 w}{\partial z^2}, \\ \frac{\partial \vartheta}{\partial t}+u\frac{\partial \vartheta}{\partial r}+w\frac{\partial \vartheta}{\partial z} &= \alpha w+\frac{v}{r}\frac{\partial}{\partial r}r\frac{\partial \vartheta}{\partial r}+v\frac{\partial^2 \vartheta}{\partial z^2}, \\ \frac{\partial ur}{\partial r}+\frac{\partial wr}{\partial z} &= 0, \end{aligned}\right\} \tag{2.1}$$

where t is time; r, z are the cylindrical radial and vertical coordinates (the z-axis is directed upwards); u, w are the radial and vertical components of velocity, respectively; ϑ is the temperature deviation from its value $\theta = \theta_0 - \gamma z$ in an undisturbed atmosphere; $\lambda = g/\theta_0$, g being acceleration due to gravity; v is the molecular or turbulent viscosity factor; $\alpha = \gamma - \gamma_0, \gamma$ being the lapse rate of the undisturbed atmosphere; and γ_0 is the dry adiabatic lapse rate.

Note that (2.1) has terms which allow for the influence of vertical turbulent viscosity. An analysis shows that these terms must be smaller than the other terms by a factor of $\varepsilon = [l(t)/h(t)]^2$ (l, h are the horizontal and vertical sizes of a thermal determined by solving the problem). However, they are included for the following reasons: first, an investigation of the balance between the inertial and viscous forces is the purpose of this paper and, secondly, elimination of terms with the higher derivative changes the type of equations, which is inadmissible here. Nevertheless, solutions taking into account and not taking into account vertical turbulent viscosity should not differ essentially from each other, because otherwise the simplifications taken are not valid.

Let us specify the initial conditions for equations (2.1). Assume that there are no motions at $t = 0$ and the appearance of thermals is simulated by specification of several axially symmetric thermal pulses located on the vertical axis at the initial moment of time:

$$\text{at} \qquad t = 0, \qquad \vartheta = \frac{4v^2}{\lambda r_0^2}\exp\left(-\frac{r^2}{2r_0^2}\right) f_0(z), \qquad w = 0, \tag{2.2}$$

where $f_0(z)$ is a function which defines the vertical distribution of ϑ. It is a non-zero function on several segments not contacting each other.

3. Solutions of the problem

Let us solve the Cauchy problem for (2.1) with the initial conditions (2.2). The solution is sought in the following form (see Malbackov 1992 for details):

$$w = 4v^2 a(t)\varphi(t) f(z,t)\exp\left(-\frac{ar^2}{2}\right), \tag{3.1}$$

$$u = -\frac{4v^2\varphi}{r}\left(1-\exp\left(-\frac{ar^2}{2}\right)\right)\frac{\partial f}{\partial z}, \tag{3.2}$$

$$\vartheta = \frac{4v^2 a\varphi_1(t)}{\lambda} f(z,t)\exp\left(-\frac{ar^2}{2}\right), \tag{3.3}$$

$$\varphi = \begin{cases} t & \text{at} \quad \alpha = 0 \\ \sin[(-\alpha\lambda)^{1/2}t]/(-\alpha\lambda)^{1/2} & \text{at} \quad \alpha < 0 \\ \sinh[(\alpha\lambda)^{1/2}t]/(\alpha\lambda)^{1/2} & \text{at} \quad \alpha > 0, \end{cases} \tag{3.4}$$

$$\varphi_1 = \begin{cases} 1 & \text{at} \quad \alpha = 0 \\ \cos[(-\alpha\lambda)^{1/2}t] & \text{at} \quad \alpha < 0 \\ \cosh[(\alpha\lambda)^{1/2}t] & \text{at} \quad \alpha > 0, \end{cases} \tag{3.5}$$

$$a = 1/(2vt + r_0^2); \tag{3.6}$$

$f(z,t)$ satisfies the equation

$$\frac{\partial f}{\partial t} + 4v^2 a\varphi f \frac{\partial f}{\partial z} = v\frac{\partial^2 f}{\partial z^2}; \tag{3.7}$$

at

$$t = 0, \qquad f = f_0(z). \tag{3.8}$$

If we assume a neutral stratified atmosphere ($\alpha = 0, r_0 = 0$) and substitute φ, a from (3.4), (3.6) into (3.7), we obtain a problem for the linear thermal pulse distributed randomly along the axis Oz:

$$\frac{\partial f}{\partial t} + 2vf\frac{\partial f}{\partial z} = v\frac{\partial^2 f}{\partial z^2}; \tag{3.9}$$

at

$$t = 0, \quad f = f_0(z). \tag{3.10}$$

Equation (3.9) is the well-known Burgers equation, which is reduced to the linear equation using the substitution

$$f = F(z,t)\Big/\left(c + \int_z^\infty F\,\mathrm{d}z\right).$$

As a result, we have the following problem:

$$\frac{\partial F}{\partial t} = v\frac{\partial^2 F}{\partial z^2}; \tag{3.11}$$

at

$$t = 0, \quad F = cf_0 \exp \int_z^\infty f_0 \,\mathrm{d}z. \tag{3.12}$$

4. Coagulation of convective cells

Let us study in more detail thermal convection caused in the following way: finite amounts of heat q are instantaneously released at $t = 0$ at several fixed points of space on the axis with the coordinates $z = z_i$ ($i = 1, 2, \ldots, n; z_{i+1} > z_i$). The solution to the problem for this case was obtained in Malbackov (1992):

$$f = \frac{\sum_{i=1}^{n} b_i \exp(-\eta_i^2)}{2(\pi vt)^{1/2}\left(1 + \sum_{i=1}^{n} b_i\psi(\eta_i)\right)}, \tag{4.1}$$

where

$$\eta_i = \frac{(z - z_i)}{2(vt)^{1/2}}, \quad \psi(\eta_i) = \frac{1}{\pi} \int_{\eta_i}^{\infty} \exp(-\alpha^2)\, \mathrm{d}\alpha,$$

$$b_1 = \exp(Q_1) - 1, \quad b_j = \exp\left(\sum_{i=1}^{j} Q_i\right) - \exp\left(\sum_{i=1}^{j-1} Q_i\right) \ (j = 2, \ldots, n),$$

$$Q_i = \frac{\lambda q_i}{8\pi c_p \rho v^2}, \quad \sum_{i=1}^{n} Q_i = Q_s = \frac{\lambda q_s}{8\pi c_p \rho v^2}, \quad Q_s = \int_{-\infty}^{\infty} f \mathrm{d}z.$$

Here Q_i, Q_s are dimensionless constants; c_p is the heat capacity of air at constant pressure; ρ is its mean density.

Relation (4.1) results from the condition of conservation of the amount of heat released at the initial moment:

$$2\pi \int_0^{\infty} \int_{-\infty}^{\infty} \vartheta\, \mathrm{d}zr\, \mathrm{d}r = \frac{q_s}{c_p \rho}. \tag{4.2}$$

Now let us determine the parameters of the problem for which the simplifications of the vertical boundary layer are valid. Since the last term in (3.9) which allows for the influence of vertical turbulence is small, the solution (4.1) should be close to the solution to problem (3.9) to a sufficient accuracy:

$$\frac{\partial f}{\partial t} + 2vf \frac{\partial f}{\partial z} = 0, \quad \int_{-\infty}^{\infty} f \mathrm{d}z = Q_s. \tag{4.3}$$

At $n = 2$, the solution to problem (4.3) has the following form:
at

$$0 \leqslant t \leqslant t_1 = (z_2 - z_1)^2 / 4vQ_1$$

$$f = \begin{cases} (z - z_1)/2vt & \text{at} \quad z_1 \leqslant z \leqslant h_1(t) = z_1 + 2(Q_1 vt)^{1/2} \\ (z - z_2)/2vt & \text{at} \quad z_2 \leqslant z \leqslant h_2(t) = z_2 + 2(Q_2 vt)^{1/2} \\ 0 & \text{at} \quad z < z_1, z > h_2; \end{cases} \tag{4.4}$$

at

$$t_1 < t \leqslant t_2 = t_1 (Q_s^{1/2} + Q_2^{1/2})^2 / Q_1$$

$$f = \begin{cases} (z - z_1)/2vt & \text{at} \quad z_1 \leqslant z \leqslant h_1(t) = \frac{1}{2}(z_2 + z_1) + 2Q_1 vt/(z_2 - z_1), \\ (z - z_2)/2vt & \text{at} \quad h_1 < z \leqslant h_2(t) = z_2 + 2(Q_2 vt)^{1/2}, \\ 0 & \text{at} \quad z < z_1, z > h_2; \end{cases} \tag{4.5}$$

at

$$t > t_2$$

$$f = \begin{cases} (z - z_1)/2vt & \text{at} \quad z_1 \leqslant z \leqslant h_1(t) = z_1 + 2(Q_s vt)^{1/2}, \\ 0 & \text{at} \quad z < z_1, z > h_1. \end{cases} \tag{4.6}$$

A comparison of the solutions allowing for and not allowing for vertical viscosity shows that it has minor influence on the process, when $Q_i = \lambda q_i / \ (8\pi c_p \rho v^2) \geqslant 10$. The vertical scales of the process prevail over the horizontal scales only at such parameter values. For example, figure 1 shows the forms of functions $f(z)$, which do and do not

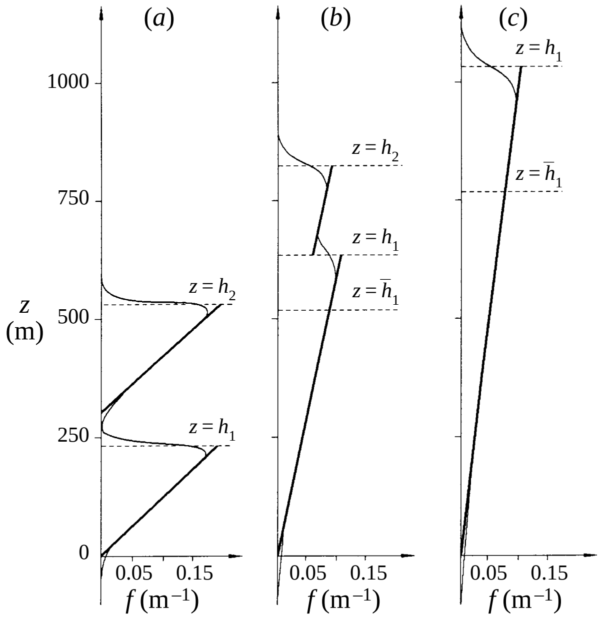

FIGURE 1. The functions $f(z)$ at different moments of time with the following parameter values: $n = 2, Q_1 = Q_2 = 25; \nu = 10$ m^2 s^{-1}. Thin line, the solution (4.1) accounting for vertical viscosity; bold line, the solution (4.4)–(4.6) not accounting for vertical viscosity; $z = h_1$ and $z = h_2$ are the maximal vertical size of thermals; $z = \bar{h}_1$ is the maximal vertical size of the lower thermal when the upper thermal is absent.

account for vertical viscosity at different moments of time at the following values of the parameters:

$$n = 2, \quad Q_1 = Q_2 = 25, \quad z_1 = 0, \quad z_2 = 600 \text{ m}, \quad \nu = 10 \text{ m}^2 \text{ s}^{-1}. \tag{4.7}$$

It can be seen that, at $Q_1 = Q_2 = 25$, the influence of vertical turbulence is not large. An analysis of the solution to (4.4)–(4.6) shows that the whole process can be arbitrarily divided into three stages beginning at $t = 0$, $t = t_1$ and $t = t_2$. Relations (4.4) are valid at the first stage. Thermal convection at $0 \leqslant t \leqslant t_1$ develops in two regions, which are not adjacent to each other, i.e. thermals do not interact with each other. At this time, u is small in all convective areas, does not depend on z, and w grows with height, in accordance with the linear law. It reaches its maximum values

$$w_i = 2(Q_i\nu/t)^{1/2} \quad \text{at} \quad r = 0 \quad \text{and} \quad h_i = 2(Q_i\nu t)^{1/2} + z_i, \quad i = 1, 2, \tag{4.8}$$

on the axis near the upper boundaries of thermals. It reaches its minimum values $w = w_{min}$ at their lower boundaries: $z = z_i + w_{min}t$. Here $w < w_{min}$ are the velocities which are negligibly small for thermals. In this case, the velocities of ascent of the upper boundaries are smaller than the maximum values of updraughts in thermals.

Now let us consider the results of observations of ascending thermals. It is known that in real conditions thermals increase in volume during ascent (Andreev & Pantchev 1975; Ludlam & Scorer 1952). Laboratory experiments show linear variation of thermal radii with height (Wilkins, Sasaki & Marion 1972). The vertical component of motion is prevailing in thermals; it is maximum in the upper part of a cell, which is called the core. Motions are insignificant in the lower part of a thermal. The ascent velocity of the core is always lower than the maximum vertical motions in it (Andreev & Pantchev 1975). A comparison of the results of observations with theoretical results shows that the solution obtained describes qualitatively the main features of the distribution of fields of meteorological elements in thermals.

Let us dwell on the mechanism of interaction of thermals. The stage of interaction begins at $t = t_1$. At this time, the upper boundary of the lower thermal reaches the level $z = z_2$ and increases its velocity. Thus, the velocity of movement of an isolated thermal decreases with time: $\mathrm{d}h_1/\mathrm{d}t = (Q_1 \nu/t)^{1/2}$, whereas during the interaction this velocity is constant and $\mathrm{d}h_1/\mathrm{d}t = 2\nu Q_1/(z_2 - z_1)$. The ascent velocity of the lower thermal increases due to its interaction with the upper thermal. The same conclusion has been obtained experimentally (Wilkins *et al.* 1972). As the velocity of the upper boundary of the upper thermal also decreases with time ($v_2 = \mathrm{d}h_2/\mathrm{d}t = (Q_2 \nu/t)^{1/2}$), the lower thermal absorbs the upper thermal completely. This takes place at $t = t_2$. A new thermal formed at this time does not differ from the thermal formed under the influence of one pulse with the power $q_s = q_1 + q_2$ given at $t = 0,\ r = 0,\ z = z_1$. Note that the coagulation of thermals is caused by the action of nonlinear dynamic factors: linearization of equations is inadmissible, because in this case no coagulation of thermals can take place due to the principle of superposition. For example, a lower and more powerful thermal can go through the upper one, and after that the two thermals will again exist independently.

Therefore, the processes of dynamic entrainment are an important factor causing growth of convective cells. Ludlam & Scorer (1952) came to the same conclusion. In accordance with their investigations, the total mass of entrained thermals can substantially exceed the mass of the mother cell. As a result, the mother cell rises. It will be shown below that the interaction processes can lead not only to growth of thermals but also to their destruction.

Unfortunately, we know of no data of natural observations of the interaction of atmospheric thermals. The results of experiments on laboratory simulations of such processes are presented in Wilkins *et al.* (1972): portions of a fluid lighter in weight than water (a water solution of a special chemical) were injected into water at equal time intervals. As a result, thermals with the same buoyancy and ascending along the same path were obtained. Thus, a system consisting of three interacting thermals located over each other was formed. The experiments have shown that the upper boundary of the first thermal rose at the rate $v \sim 1/t^{-1/2}$. The second thermal moved upward at a greater speed than the first thermal. However, the upper boundary of the third and the lowest thermal moved at a speed equal to that of the second thermal.

Let us compare the conclusions obtained experimentally with the theoretical results. For this purpose, we take the solution to the problem without vertical turbulence, which describes the interaction of three similar ($Q_1 = Q_2 = Q_3 = Q_s/3$) thermals located at equal intervals ($z_2 - z_1 = z_3 - z_2$):

$$f = \begin{cases} (z - z_1)/2\nu t & \text{at} \quad z_1 \leqslant z \leqslant h_1 \\ (z - z_2)/2\nu t & \text{at} \quad h_1 < z \leqslant h_2 \\ (z - z_3)/2\nu t & \text{at} \quad h_2 < z \leqslant h_3 \\ 0 & \text{at} \quad z < z_1, \quad z > z_3, \end{cases}$$

where

$$h_1 = \frac{2Q_1 \nu t}{z_2 - z_1} + \frac{z_2 - z_1}{2}, \quad h_2 = \frac{2Q_1 \nu t}{z_3 - z_2} + \frac{z_3 - z_2}{2},$$

$$h_3 = 2(Q_3 \nu t)^{1/2} + z_3, \quad t_1 = \frac{(z_2 - z_1)^2}{4\nu Q_1}, \quad t_2 = t_1(3 + 2\sqrt{2}).$$

This solution is valid in a time interval $t_1 < t < t_2$, where t_1 corresponds to the time, when the lower thermal 'catches up with' the middle thermal. At the same moment, the core of the middle thermal enters the trace of the upper thermal. The time t_2 corresponds to when the upper thermal coalesces with the middle thermal.

Now let us determine the ascent velocities of the upper boundaries of thermals. It is easily seen that the vertical propagation speed of the upper thermal decreases: $v_3 = \mathrm{d}h_3/\mathrm{d}t \sim t^{-1/2}$ and that the middle thermal rises quicker than the upper thermal: $v_2 = \mathrm{d}h_2/\mathrm{d}t = 2\nu Q_2/(z_3 - z_2)$. However, the speed of the upper boundary of the lower thermal is the same as that of the middle thermal: $v_1 = v_2$. Thus, this model describes what has been established experimentally.

Let us investigate the evolution of thermals in a stably ($\alpha < 0$) and unstably ($\alpha > 0$) stratified atmosphere. The range of external parameter values for which our theory is applicable determines the similarity between the solutions to (3.7), (3.8) and to the following problem without turbulent viscosity:

$$\frac{\partial f}{\partial t} + 4\nu^2 a\varphi f \frac{\partial f}{\partial z} = 0, \quad \text{at} \quad t = 0 \quad f = f_0(z). \tag{4.9}$$

The solutions to (4.9) at $\alpha < 0$ and at $\alpha > 0$ for one thermal pulse are obtained in Malbackov (1972). The solution in the stable atmosphere (as well as at $\alpha = 0$) is valid only when thermal pulses are sufficiently strong. In contrast to neutral stratification, however, the thermal core reaches a maximum height long before the complete decay of convection. Once growth in the vertical has stopped, the horizontal size of a thermal gradually approach its vertical size. For this reason, the applicability of the theory for $\alpha < 0$ is also bounded in time. At $\alpha > 0$, the strength of the initial thermal pulse is not substantial, because thermal convection is maintained by the energy of instability, and the simplifications of the vertical boundary layer are valid. The reason is more rapid increase of the vertical scales than the horizontal scales.

It is not difficult to obtain the solutions to (4.9) at $\alpha > 0$ and $\alpha < 0$ and for the case of two thermal pulses. An analysis of these solutions (we do not present them here, because they are cumbersome) shows that the character of interaction of thermals is about the same as at $\alpha = 0$. The difference from the case $\alpha = 0$ is that the interaction takes place either quicker (at $\alpha > 0$) or slower (at $\alpha < 0$) due to more rapid or slower increase of the vertical size of thermals.

5. Instability of convective cells

Let us show that relations (4.1) lose their physical meaning at certain critical values of the parameters due to disturbance of the balance between the inertial and viscous forces. Let us determine the critical values of the parameters and investigate the behaviour of the function f at the parameter values that are close to critical values. In considering the case of the influence of two thermal pulses on the atmosphere, we assume that the first pulse is caused by a powerful thermal influence at $Q_1 > 10$, and the second very weak thermal influence at $Q_2 = \varepsilon \ll 1$ is caused by random fluctuations in the temperature field. In this case we have $b_1 = \exp(Q_1) - 1 \approx \exp(Q_1)$, $b_2 = \exp(Q_1 + \varepsilon) - \exp(Q_1) \approx \varepsilon \exp(Q_1)$. After substituting b_1 and b_2 into (4.1), we have

$$f = \frac{\exp(Q_1)(\exp(-\eta_1^2) + \varepsilon \exp(-\eta_2^2))}{2(\pi v t)^{1/2}(1 + \exp(Q_1)(\psi(\eta_1) + \varepsilon\psi(\eta_2)))}. \tag{5.1}$$

The denominator in (5.1) vanishes, and the solution makes no sense at

$$\varepsilon = -\frac{\exp(-Q_1) + \psi(\eta_1)}{\psi(\eta_2)}. \tag{5.2}$$

Thus, ε depends on t, t_1, z, z_1, z_2, but as the fluctuations in the temperature field can appear at any moment of time and at any point of space, the minimum absolute value of ε should be taken from (5.2). This value corresponds to a thermal fluctuation of minimum strength to destroy the thermal. It is reached at $\psi(\eta_1) = \psi(-\infty) = 1$ and $\psi(\eta_2) = \psi(\infty) = 0$. Substituting these values into (5.2), we finally have

$$\varepsilon = \varepsilon_{cr} = -\exp(-Q_1). \tag{5.3}$$

Weaker fluctuations do not destroy the thermal. It is easily seen that $f \to 0$ at $\eta_1 \to \infty$, $\eta_2 \to -\infty$. But the numerator in (5.1) vanishes quicker than the denominator at certain space points, which depend on z_1 and z_2 at $\varepsilon \to \varepsilon_{cr}$.

A numerical solution to the problem without the simplifications of the theory of vertical boundary layers, which has been obtained by us but is not published, shows that a process like wave turnover with subsequent dissipation of a cell under the influence of entrainment of the surrounding air into the cell is a result of disturbance of the stability. In this simplified model, 'wave turnover' is prohibited by the form of the solution itself, and the absence of solution is interpreted as instantaneous destruction of the cell.

Let us define the maximum size of convective cells. For this purpose, consider relation (5.3): it shows that the stronger the initial influence on the atmosphere, the weaker the hydrodynamic stability of the convective formation it causes. If a convective cell is formed by coalescence of several thermals, the more heat contained in the region of convection the weaker is the stability of a convective cell.

If we consider that air viscosity is molecular, we have $v \approx 2 \times 10^{-5}\,\mathrm{m}^2\ \mathrm{s}^{-1}$ and $\lambda = 0.033\,\mathrm{m\ s}^{-2}\ {}^0K$, $\rho = 10^3\mathrm{g\ m}^{-3}$, $Q_1 = 25$. Then, as can be easily calculated by (4.1), (5.3), a thermal perturbation equal to $q_2 = -4 \times 10^{-10}$cal is sufficient for a microscale convective cell to lose its stability. Random perturbations on such a scale can be realized even due to thermal motion of molecules.

If a medium is considered to be turbulent, turbulent pulsations in the temperature field with $q_2 = -1$ cal lead to 'destruction' of a convective cell at $v = 10\ \mathrm{m}^2\ \mathrm{s}^{-1}$ and $Q_1 = 25$. Naturally, such a cell is very close to an unstable cell. As Q_1 increases, instability increases greatly. For example, at $Q_1 = 100$ effects that are 30 orders of magnitude smaller than at $Q_1 = 25$ cause 'destruction' of a cell.

It can be easily shown using the solutions obtained that the vertical size h is related to the horizontal size l of thermals as

$$n = h/l = Q_1^{1/2}. \tag{5.4}$$

Relation (5.4) shows that the greater the difference between the vertical and the horizontal scales of a convective cell, the weaker is its inertial stability. Actually, observations show that convective cells with approximately the same vertical and horizontal size are encountered more often (Wolfson 1961; Mazin & Shmeter 1983).

Thus, the theory proposed is applicable in the following range of Q_s values:

$$10 \leqslant Q_s \leqslant Q_c \approx 25. \tag{5.5}$$

At $Q_s < 10$, h and l differ insignificantly. Hence, the simplifications of the vertical boundary layer that we used during the derivation of the initial equations are not applicable. The cell is unstable at $Q_s > Q_c$.

Let us determine the maximum scales of convective turbulent pulsations and the maximum scales of thermals using (5.5). Assuming that $i = 1$, $Q_1 = Q_c$, $z_1 = 0$ in (4.8), we have

$$t_c = 4Q_c \nu / w_m^2, \quad h_c = 2(Q_c \nu t_c)^{1/2}, \tag{5.6}$$

where t_c is the time of development of a convective cell; w_m is the minimum value of vertical velocity in a cell for the convective formations of this type; h_c is the characteristic vertical scale of a cell.

Assuming that the molecular viscosity of air is $\nu = 2\times10^{-5}$ m^2 s^{-1} at $Q_c = 25$, $w_m = 10^{-2}$ m^{-1}, we have $t_c = 20$ s, $h_c = 0.2$ m. In fact, thermal turbulence is not observed in the atmosphere in the pure state: convective pulsations cannot be separated from pulsations caused by many other factors. It is known, however, that the length of a laminar thermal jet over a smouldering cigarette in immobile air is 10–20 cm, which agrees with the value of h obtained theoretically. Higher, the jet breaks up into separate vortex formations of smaller sizes. And although the jet over a cigarette is not described by the solutions obtained, it is a prominent example of an unstable thermal formation, whose vertical size is larger than its horizontal size, and the shape is close to an axially symmetric one. Therefore, it is reasonable to consider that the properties of a thermal jet over a cigarette are close to the properties of convective cells. A turbulent medium, where thermals originate, is formed by thermally induced pulsations and turbulent perturbations caused by shear instability of the external flow.

Assuming that a medium is turbulent (at $\nu = 10$ m^2 s^{-1} and $w_m = 1$ m s^{-1}), we have the following maximum values of space-time scales of thermals: $h_c = 10^3$ m, $t_c = 10^3$ s. The values obtained are supported by observations.

Note, however, that in real conditions a cell reaches its maximum size at the stage of maximum evolution, whereas in accordance with (5.6) this occurs at the stage of the process dissipation. This can be explained in a simple way: as a rule, real thermals develop spontaneously due to the energy of instability. Relations (5.6) do not take into account the influence of stratification on the process. Let us estimate this influence on the evolution of convective cells. Characteristic time scales of gravitational waves (at $a < 0$) and the time of their existence (at $a > 0$) are determined by the Brunt–Väisälä frequency:

$$t_b = 2\pi/(\mid \alpha \mid \lambda)^{1/2}. \tag{5.7}$$

Substituting $\alpha = 3 \times 10^{-3}$ and -3×10^{-3} K m^{-1}, which correspond to unstable and stable stratifications of air, into (5.7), we have $t_b \cong 600$ s at $\lambda = 0.033$ m s$^{-2} K^{-1}$. In the case of molecular viscosity of air, $t_c \ll t_b$. Thus, stratification of air does not influence the scales of convective pulsations, which generate atmospheric turbulence. A thin surface layer, where the value of α can be 2–3 orders of magnitude larger than its characteristic value, is an exception. This property is taken into account in the known parameterizations of the constant flows of the atmospheric layer (Deardorff 1974).

In the case of a turbulent atmosphere, we have $t_c > t_b$. Hence, stratification of air is of considerable importance in the formation of thermals.

6. Convection in the conditions of unstable stratification of the atmosphere

Assuming that $\alpha > 0$, $r_0 = 0$ in (3.4), (3.6) and substituting their values into (3.7), we have

$$\frac{\partial f}{\partial t} + \frac{2\nu \sinh((\alpha\lambda)^{1/2}\, t)}{(\alpha\lambda)^{1/2}\, t} f \frac{\partial f}{\partial z} = \nu \frac{\partial^2 f}{\partial z^2}. \tag{6.1}$$

The function f must satisfy the following integral condition:

$$\int_{-\infty}^{\infty} f \, \mathrm{d}z = Q_\varepsilon, \quad Q_\varepsilon = \frac{\lambda q_\varepsilon}{8\pi c_p \rho \nu^2}, \tag{6.2}$$

where q_ε is the amount of heat released at $t = 0$. The total amount of heat in the region of convection increases with time:

$$\frac{q_s}{c_p \rho} = 2\pi \int_0^{\infty} \int_{-\infty}^{\infty} \vartheta \, \mathrm{d}z r \mathrm{d}r = \frac{q_\varepsilon \cosh((\alpha\lambda)^{1/2}\, t)}{c_p \rho}. \tag{6.3}$$

Problem (6.1), (6.2) is solved numerically. Several numerical schemes are used and all of them are no longer stable at $t > t_c$. The start of instability and 'the form' of its realization depend on the scheme chosen. However, this dependence is weak with sufficiently small time-space steps; in this case, instability takes place at Q_s ranging from 25 to 100:

$$Q_s = Q_c = Q_\varepsilon \cosh((\alpha\lambda)^{1/2}\, t) \approx 25\text{–}100. \tag{6.4}$$

A comparison of (5.5) and (6.4) allows us to conclude that whatever the stratification of the atmosphere, a convective cell remains stable only when the amount of heat contained in it does not exceed some critical value determined by relations (5.5), (6.4).

The numerical solution of problem (6.1), (6.2) is in good agreement with the analytical solution of problem (4.9) in Malbackov & Perov (1993), which corresponds to $\alpha > 0$ for the case when vertical viscosity is neglected. The approximate form of this solution at $t \gg 1/(\alpha\lambda)^{1/2}$ is as follows:

$$\left.\begin{array}{ll}
\text{at} & 0 \leqslant z \leqslant h, \quad h = 2(Q_\varepsilon \nu \exp((\alpha\lambda)^{1/2}\, t)/(\alpha\lambda)^{1/2})^{1/2}, \\
& w = (\alpha\lambda)^{1/2}\, z \exp(-ar^2/2), \quad \vartheta = \alpha z \exp(-ar^2/2), \\
& u = -(2\nu/r)(1 - \exp(-ar^2/2)); \\
\text{at} & z < 0, \text{ and } z > 0, \quad w = u = \vartheta = 0.
\end{array}\right\} \tag{6.5}$$

Expressions for the critical velocity w_c, the maximum height of the convective cell h_c, and the time of existence of the cell t_c obtained with the help of (6.4), (6.5) have the following form:

$$t_c = \frac{1}{(\alpha\lambda)^{1/2}} \ln\left(\frac{Q_c}{Q_\varepsilon}\right), \quad h_c = 2\left(\frac{Q_c \nu}{(\alpha\lambda)^{1/2}}\right)^{1/2}, \quad w_c = 2\left(Q_c \nu (\alpha\lambda)^{1/2}\right)^{1/2}. \tag{6.6}$$

Assuming that $\alpha = 3 \times 10^{-3}$ K m^{-1}, $\lambda = 0.033$ m s^{-2} K^{-1}, $\nu = 10$ m^2 s^{-1}, $Q_c = 25$, and substituting these values into (6.6), we obtain $h_c \cong 320$ m, $w_c \cong 1.6$ m s^{-1}, which is close to the value observed in real thermals.

It should be noted that air motions within the atmospheric boundary layer are very diverse and spontaneous. The theory developed here does not describe all the diversity of forms of atmospheric convective cells, but it qualitatively explains the reason for this diversity. This implies that all well-developed cells are unstable relative to finite perturbations. The theory does not give an answer to the question of what is the mechanism of instability. It is, however, different for cells of different intensity. The reason for the beginning of the destruction of cells is also different. 'Powerful' cells are unstable relative to very weak perturbations caused by random fluctuations in the temperature field. Weaker thermals can break down as a result of their interaction with descending cells. There can be many other reasons for the instability which are not considered by this simplified model. For example, there are the processes of interactions of cells with each other and with the environment, which take place at the periphery of thermals. Nonetheless, the processes mentioned, such as dissipation, spontaneous growth and interaction of thermals, cause diversity of forms of motions in the convective boundary layer. Nonlinear interaction causes both the growth and the destruction of thermals.

7. Statistical characteristics of an ensemble of thermals

The results obtained allow us to propose the following hypothesis for the distribution of thermals. We investigate the stability of thermals with positive buoyancy: $Q_s > 0$. Let us consider an unstable atmosphere again. At $\alpha > 0$, the buoyancy of thermals increases with time due to the energy of instability. We assume that buoyancy increases from Q_s to $Q_s + \mathrm{d}Q_s$. Then, in accordance with (5.3), the probability that at such an increase of its buoyancy a cell will retain its stability, is as follows:

$$S(Q_s)\,\mathrm{d}Q_s = \exp(-Q_s)\,\mathrm{d}Q_s, \tag{7.1}$$

when the following condition is fulfilled:

$$\int_0^\infty \exp(-Q_s)\,\mathrm{d}Q_s = 1, \tag{7.2}$$

where $S(Q_s)$ is the density of distribution of cells over Q_s.

If the theory is correct at $Q_s \geqslant Q_\varepsilon$, we have, in place of (7.1), (7.2), the following:

$$S(Q_s)\,\mathrm{d}Q_s = \exp(Q_\varepsilon - Q_s)\,\mathrm{d}Q_s, \quad \int_{Q_\varepsilon}^\infty \exp(Q_\varepsilon - Q_s)\,\mathrm{d}Q_s = 1. \tag{7.3}$$

For the calculations, it is more convenient to write $S(h)$ in terms of the vertical size of thermals, or the time of their existence $S(t)$, or the frequencies of oscillations $S(n)$, where $n = 1/t$. For this purpose, we use (6.3) and (6.5)

$$Q_s = Q_\varepsilon \cosh\left((\alpha\lambda)^{1/2} t\right) \approx Q_\varepsilon \exp\left((\alpha\lambda)^{1/2} t\right), \quad h = 2\left(\frac{\nu Q_s}{(\alpha\lambda)^{1/2}}\right). \tag{7.4}$$

Using the relations between Q_s and h, Q_s and t, Q_s and n we have, in place of (7.1), the expressions

$$S(h)\,\mathrm{d}h = \frac{h}{h_0^2}\exp\left(-\frac{h^2}{2h_0^2}\right)\mathrm{d}h, \quad h_0 = \left(\frac{2\nu}{(\alpha\lambda)^{1/2}}\right)^{1/2}, \tag{7.5}$$

$$S(t)\,\mathrm{d}t = Q_\varepsilon(\alpha\lambda)^{1/2}\exp\left((\alpha\lambda)^{1/2}t - Q_\varepsilon\exp\left((\alpha\lambda)^{1/2}\,t\right)\right)\mathrm{d}t, \tag{7.6}$$

$$S(n)\,\mathrm{d}n = -\frac{Q_\varepsilon(\alpha\lambda)^{1/2}}{n^2}\exp\left(\frac{(\alpha\lambda)^{1/2}}{n} - Q_\varepsilon\exp\left(\frac{(\alpha\lambda)^{1/2}}{n}\right)\right)\mathrm{d}n. \tag{7.7}$$

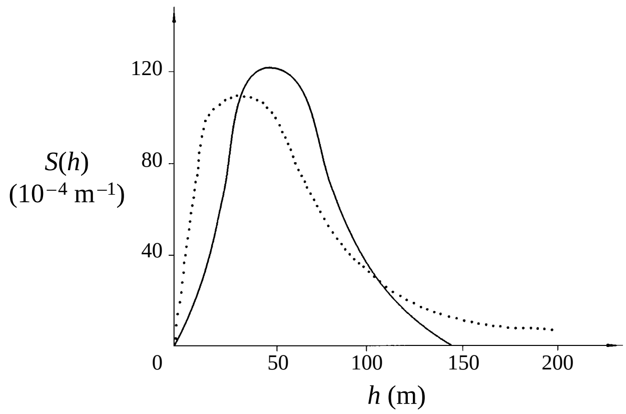

FIGURE 2. Comparison of calculations with observation data. Distributions of cell sizes: solid line, calculations with (7.5)

Obviously, expression (7.5) is most convenient, because in this case the spectral density of the size distribution of thermals is

$$hS(h) = \left(\frac{h}{h_0}\right)^2 \exp\left(-\frac{h^2}{2h_0^2}\right). \tag{7.8}$$

Also, to make a comparison with the data from observations, we need the following quantities: $S_{\bar{\vartheta}}(h), S_{\bar{w}}(h), S_{\overline{w\vartheta}}(h)$, where $\bar{w}, \bar{\vartheta}$ are the vertical velocity and the excess temperature due to combined action of thermals. Let us introduce definitions of these quantities.

Let ΔS be a grid cell of a large-scale model. Let this cell contain N thermals, whose interaction is neglected. First we should determine $S_{\bar{\vartheta}}(h)$, where $\bar{\vartheta}$ is the excess temperature in the cell due to the combined action of thermals. The area of the horizontal section of thermals is assumed to be much smaller than $\Delta S : \pi r_0^2 \ll \Delta S$, where $r_0 = (5/a)^{1/2}$. It is assumed that all thermals appear simultaneously at $t = 0$. They spontaneously grow and break down at $t = \Delta t$, where Δt is the time step of the large-scale model. Convection does not reach 'saturation', i.e. $\Delta S = \pi r_0^2 N$. Thus, the model is ready for parameterization. The whole cycle is repeated with changed large-scale parameters in the time period Δt (see Kuo 1965, 1974 for details).

Using ϑ from (6.5), $S(h)$ from (7.5) and averaging over ΔS, we have

$$S_{\bar{\vartheta}}(h) = \frac{2\pi N\alpha}{\Delta S} hS(h) \int_0^{r_0} \exp\left(-\frac{r^2}{2}\right) r\mathrm{d}r \cong \frac{\alpha(\pi)^{1/2}h^2}{10h_0^2} \exp\left(-\frac{h^2}{2h_0^2}\right). \tag{7.9}$$

It can also be shown that

$$S_{\bar{w}}(h) \cong \frac{(\pi\alpha\lambda)^{1/2}h^2}{10h_0^2} \exp\left(-\frac{h^2}{2h_0^2}\right), \tag{7.10}$$

$$S_{\overline{w\vartheta}}(h) \cong \frac{\alpha(\pi\alpha\lambda)^{1/2}h^3}{10h_0^2} \exp\left(-\frac{h^2}{2h_0^2}\right). \tag{7.11}$$

7.1. *Comparison of calculations and observations*

A comparison of calculations and observations is illustrated in figures 2–5. In figure 2, two curves are given. The size distribution of convective cells shown by a solid

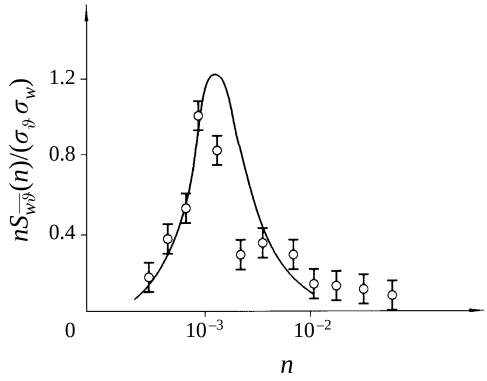

FIGURE 3. Comparison of calculations with observation data: averaged normalized spectral density of vertical heat flux at $z = 265$ m: solid line, calculations with (7.11)

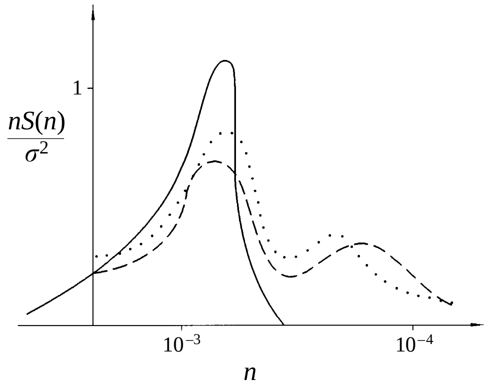

FIGURE 4. Comparison of calculations with observation data: an averaged spectrum of temperature (dotted line) and velocity (dashed line) in a layer 300 m thick (July 7, 1970); solid line, calculations with (7.7).

line is calculated with the use of (7.5) at $\alpha = 3 \times 10^{-3}$ K m^{-1}, $\lambda = 0.033$ m s^{-2} K^{-1}), $\nu = 5$ m^2 s^{-1}. The distribution obtained using the measurements of Wolfson (1961) is shown by a dotted line. Figure 3 shows $nS_{\overline{w\vartheta}}/\sigma_{\bar\vartheta}\sigma_{\bar w}$ ($\sigma_{\bar\vartheta}$, $\sigma_{\bar w}$ are the standard deviations ϑ and w) measured in Bizova, Ivanov & Garger (1989) and the same values calculated at $\alpha = 10^{-3}$ K m^{-1}), $\lambda = 0.033$ m s^{-2} K^{-1}, $Q_\varepsilon = 0,1$, $h_0 = 265$ m. Figure 4 shows the average values of $nS_{\bar\vartheta}(n)\sigma_{\bar\vartheta}$, $nS_{\bar w}(n)\sigma_{\bar w}$ (for the lower 300 m layer) measured by Bizova *et al.* (1989) and the same values calculated at $\alpha = 5\times10^{-4}$ K m^{-1}, $\lambda = 0.033$ m s^{-2} K^{-1}), $Q_\varepsilon = 0.1$ (note that $S_{\bar\vartheta}$ and $S_{\bar w}$ coincide in the model). Finally, figure 5 shows the same as figure 4 except that the measurements were made on another day, and the calculations were carried out at $\alpha = 10^{-3}$ K m^{-1}.

It is seen from figures 2–5 that the model gives a more ‘compact’ distribution as compared to the measurements. This can be explained by the limitations of the theory. Apparently, the main reason is that the low-frequency part of the spectrum, which corresponds to formations larger than thermals, is not filtered in the measurements. So, the second weaker maxima in the low-frequency part of the spectrum in figures 4, 5, as pointed out in Bizova *et al.* (1989), correspond to clouds of the type *Cu hum.* The cloud amount is 3–4 in both cases. Although the lower boundary of the clouds is at the height of about 1 km, the influence of the clouds is observed near the surface.

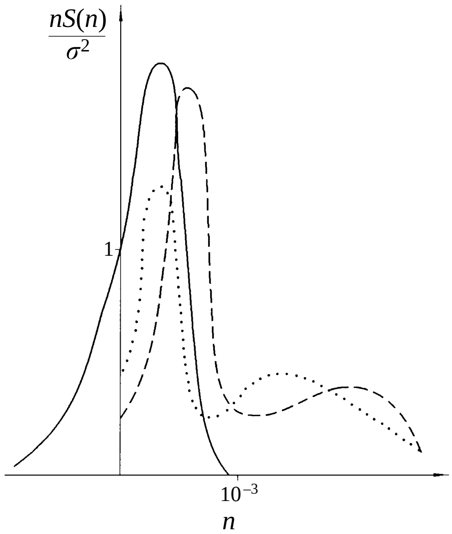

FIGURE 5. As figure 4 but data taken on August 7, 1971.

7.2. *Comparison of the analytical model with observations and calculations using the vorticity-resolving model*

A comparative analysis of the maximum vertical velocities and maximum horizontal size of thermals obtained from measurements (Konovalov 1970) and numerical results using the model of an ensemble of dry thermals is given in Vaskevitch & Pushistov 1988 (*a*, *b*). Using (7.5) and (7.6), the following relations can be obtained:

$$S(w_{max}) = \frac{w_{max}}{w_0^2} \exp\left(-\frac{w_{max}^2}{w_0^2}\right), \tag{7.12}$$

$$w_{max} = (\alpha\lambda)^{1/2}\, h, \quad w_0 = \sqrt{(2\nu\sqrt{(\alpha\lambda)^{1/2}})^{1/2}}, \tag{7.13}$$

$$S(l) = \frac{Q_\varepsilon l}{h_0^2} \exp\left(\frac{l^2}{2h_0^2} - Q_\varepsilon \exp\left(\frac{l^2}{2h_0^2}\right)\right), \quad l = 2(\nu t)^{1/2}.$$

Figures 6 and 7 illustrate the numerical and analytical results and measurements obtained by Konovalov (1970), who distinguishes two types of thermals: (*a*) thermals with a main maximum and several secondary maxima; (*b*) thermals having only one maximum. In figures 6 and 7 bold points correspond to thermals of the type (*a*), crosses denote thermals of the type (*b*), circles show numerical results. Solid lines denote analytical results at $w_0 = 1.5$ m s^{-1}, $h_0 = 150$ m, $Q_\varepsilon = 0.001$. It is seen from the figures that agreement of the results of both models with the measurements is satisfactory, but the analytical model gives a more compact distribution of thermals in accordance with their horizontal size. This may be explained by the fact that real thermals can consist of several cells located near each other, but in the analytical model thermals must be located at a large distance from each other, because their lateral interaction is not taken into account.

A comparison of theoretical results with measurements in cloud is made in Appendix B.

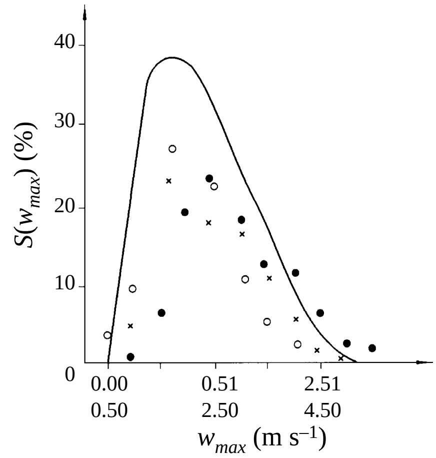

FIGURE 6. Comparison of calculations with observation data: repeatability of maximum vertical velocity of thermals; •, thermals of type (*a*); ×, thermals of type (*b*); ○, numerical model; ——, analytical model.

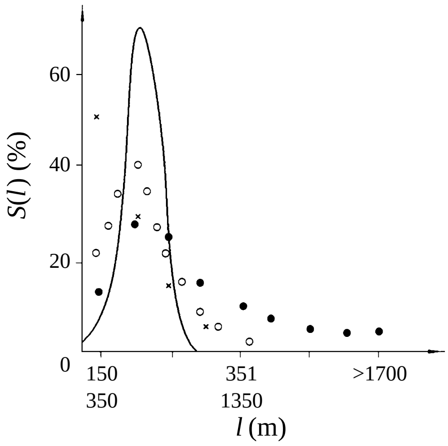

FIGURE 7. Comparison of calculations with observation data: repeatability of maximum horizontal size of thermals. The symbols are the same as in figure 6.

8. Conclusion

The results obtained in the present paper make it possible to conclude that the processes of nonlinear interaction, i.e. coagulation of cells and their instability with respect to external actions, are the reason for the disordered structure of convective ensembles. Factors of influence in numerical simulation can be neighbouring cells, as well as approximation errors: at unlimited spontaneous growth, the sensitivity of cells to perturbing factors increases without bound, and finally they collapse under the action of random factors. Computer simulation of turbulent regimes with the help of Navier–Stokes equations (Ebert *et al.* 1989; Jimenez *et al.* 1993), Boussinesq equations (Davaile & Jampart 1993; Decker *et al.* 1994; Glukhovskaya & Ordanovitch 1993; Clever & Busse 1994; Noto *et al.* 1994), as well as equations for deep (Moeng *et al.* 1995) and shallow (Andreev & Pantchev 1975; Mazin & Ckrgian 1989; Vaskevitch & Pushistov 1988 *a, b*) convection allow an assertion that an isolated pulsation is an eigensolution of the corresponding equations, and turbulence is generated by nonlinear interaction between pulsations. The present simple analytical, but not finite difference, model supports this. It should be noted, however, that since all simplifying assumptions in the problem statement are not valid for a real atmosphere, the conclusions drawn are of qualitative character, and the degree of their applicability to real atmospheres needs further verification. Besides, it is evident that although this simplified model elucidates the mechanism of formation of disordered structures with different cell sizes and different lifetimes, it does not give an answer to the question of the space-time structure of convective ensembles, which is most important in investigation of turbulent regimes. Nevertheless, the approach developed in the present paper can serve as a basis for construction of simplified spatial models of atmospheric convective ensembles, the function of which is a parameterization of convection in the simulation of weather and climate. In this case the simplifying assumptions are acceptable (see Arakawa & Schubert 1974; Kuo 1965, 1974; Tiedtke 1983, 1989). An attempt to construct a spatial model of convective ensemble was made in Malbackov & Perov (1993), where lateral interaction between cells was taken into account. It influenced only the distance between cells, but did not change their axially symmetric form.

We thank Professor Lev N. Gutman, whose ideas formed the basis of the models proposed. This work has been supported by the Soros Fund, the Russian Fundamental Research Fund, No. 94-05-16154, No. 96-05-66104 and the United States Fund ‘Man and Biosphere Program’, No. 1753-300203 R4.

Appendix A. Simplifications of the theory of vertical boundary layers

The Boussinesq equations applied to the atmosphere for an axially symmetric process, when the axis of symmetry is directed upward, have the following form (Davaile & Jampart 1993):

$$\frac{\partial u}{\partial t} + u\frac{\partial u}{\partial r} + w\frac{\partial u}{\partial z} = -R\theta\frac{\partial}{\partial r}\left(\frac{p}{P}\right) + v\frac{\partial}{\partial r}\frac{1}{r}\frac{\partial ur}{\partial r} + v\frac{\partial^2 u}{\partial z^2}, \tag{A 1}$$

$$\frac{\partial w}{\partial t} + u\frac{\partial w}{\partial r} + w\frac{\partial w}{\partial z} = -R\theta\frac{\partial}{\partial z}\left(\frac{p}{P}\right) + \lambda\vartheta + \frac{v}{r}\frac{\partial}{\partial r}r\frac{\partial w}{\partial r} + v\frac{\partial^2 w}{\partial z^2}, \tag{A 2}$$

$$\frac{\partial \vartheta}{\partial t} + u\frac{\partial \vartheta}{\partial r} + w\frac{\partial \vartheta}{\partial z} = \alpha w + \frac{v}{r}\frac{\partial}{\partial r}r\frac{\partial \vartheta}{\partial r} + v\frac{\partial^2 \vartheta}{\partial z^2}, \tag{A 3}$$

$$\frac{\partial ur}{\partial r} + \frac{\partial wr}{\partial z} = 0, \tag{A 4}$$

where R is the universal gas constant; ϑ, p are the convective deviations of temperature and pressure from their background values $\theta(z), P(z)$. The other notation is as above.

It is considered that atmospheric convection is basically a nonlinear process, and the horizontal propagation of perturbations is caused by the action of viscous forces. These assumptions imply that the terms on the left-hand sides of the Boussinesq equations, the terms taking into account the horizontal propagation of convective perturbations, as well as the terms taking into account the Archimedean force are of the same order. We introduce the following characteristic and dimensionless variables:

$$\left.\begin{aligned} t = T\tau, \quad r = L\eta, \quad z = H\zeta, \quad w = \frac{H}{T}w', \quad u = \frac{L}{T}u', \\ \vartheta = \frac{H}{T^2\lambda}\vartheta', \quad p = \frac{\nu P}{TR\theta}p', \quad L = (\nu T)^{1/2}, \quad H = nL, \quad n = \frac{H}{L}, \end{aligned}\right\} \tag{A 5}$$

where Greek symbols denote dimensionless coordinates and time, and primed symbols correspond to the sought dimensionless functions. Substituting (A 5) into (A 1–A 4), we have the following equations for the dimensionless quantities:

$$\frac{\partial u'}{\partial \tau} + u'\frac{\partial u'}{\partial \eta} + w'\frac{\partial u'}{\partial \zeta} = -\frac{\partial p'}{\partial \eta} + \frac{\partial}{\partial \eta}\frac{1}{\eta}\frac{\partial u'\eta}{\partial \eta} + \frac{L^2}{H^2}\frac{\partial^2 u'}{\partial \zeta^2}, \tag{A 6}$$

$$\frac{\partial w'}{\partial \tau} + u'\frac{\partial w'}{\partial \eta} + w'\frac{\partial w'}{\partial \zeta} = -\frac{L^2}{H^2}\frac{\partial p'}{\partial \zeta} + \vartheta' + \frac{1}{r}\frac{\partial}{\partial \eta}\eta\frac{\partial w'}{\partial \eta} + \frac{L^2}{H^2}\frac{\partial^2 w'}{\partial \zeta^2}, \tag{A 7}$$

$$\frac{\partial \vartheta'}{\partial \tau} + u'\frac{\partial \vartheta'}{\partial \eta} + w'\frac{\partial \vartheta'}{\partial \zeta} = (\alpha\lambda T^2)w' + \frac{1}{r}\frac{\partial}{\partial r}r\frac{\partial \vartheta'}{\partial \eta} + \frac{L^2}{H^2}\frac{\partial^2 \vartheta'}{\partial \zeta^2}, \tag{A 8}$$

$$\frac{\partial u'\eta}{\partial \eta} + \frac{\partial w'\eta}{\partial \zeta} = 0. \tag{A 9}$$

It follows from (A 6)–(A 9) that at $H^2 \gg L^2$ the term $(1/n^2)(\partial p'/\partial \zeta)$ in (A 7) can be omitted, which was done in (A 1)–(A 3). The last terms in (A 6)–(A 8) which are also small, are left in (A 1)–(A 3) as terms with the highest derivative determining the type of solution to the problem (A 1)–(A 4). Moreover, there is an additional guarantee of smallness of the terms with the vertical pressure gradient. It is easily seen that in the case when the simplifications of the vertical boundary layer are valid, equation (A 6) drops out of system (A 6)–(A 9) and serves to determine p'. It follows from this equation and from (6.5) that p' practically does not depend on z inside the boundary layer. Thus, the vertical pressure gradient inside the boundary layer is small at $H^2 \gg L^2$. Also, it follows from (A 8) at $T \ll (\alpha\lambda)^{1/2}$ that stratification of the atmosphere must not influence convection. The above analysis of the solutions leads to the same conclusion, which confirms the correctness of the conclusions obtained for the cells with $H^2 \gg L^2$.

Appendix B. Comparison of theoretical results with measurements in clouds

It has been shown in Malbackov 1992 that with some additional simplifying assumptions all conclusions obtained for dry convective cells can be extended to moist convective cells, i.e. convective clouds. In this case, γ_0 in the expression $\alpha = \gamma - \gamma_0$ can be considered as moist–adiabatic lapse rate. Measurements given in LeMone, Chang & Lucas (1994) (rectangles) are compared with theoretical curves in figure 8. Distribution of updraughts with the diameter of the area is shown in the upper part of the figure. The theoretical curve has been calculated using the following relation:

$$S(d) = 84\frac{Q_\varepsilon d}{h_1^2}\ \exp\left(\frac{d^2}{h_1^2} - Q_\varepsilon \exp\left(\frac{d^2}{h_1^2}\right)\right), \quad h_1 = 2\left(\nu\,(\alpha\lambda)^{1/2}\right)^{1/2}, \tag{B 1}$$

where $d = 2(\nu t)^{1/2}$ is an arbitrarily chosen diameter of the area, in which $w > w_{min}$, and $w_{min} > 0$, which can be measured; $h_1 = 0.7$ km, $Q_\varepsilon = 0.6$.

A significant difference between the theory and measurements at $d > 2$ km can be

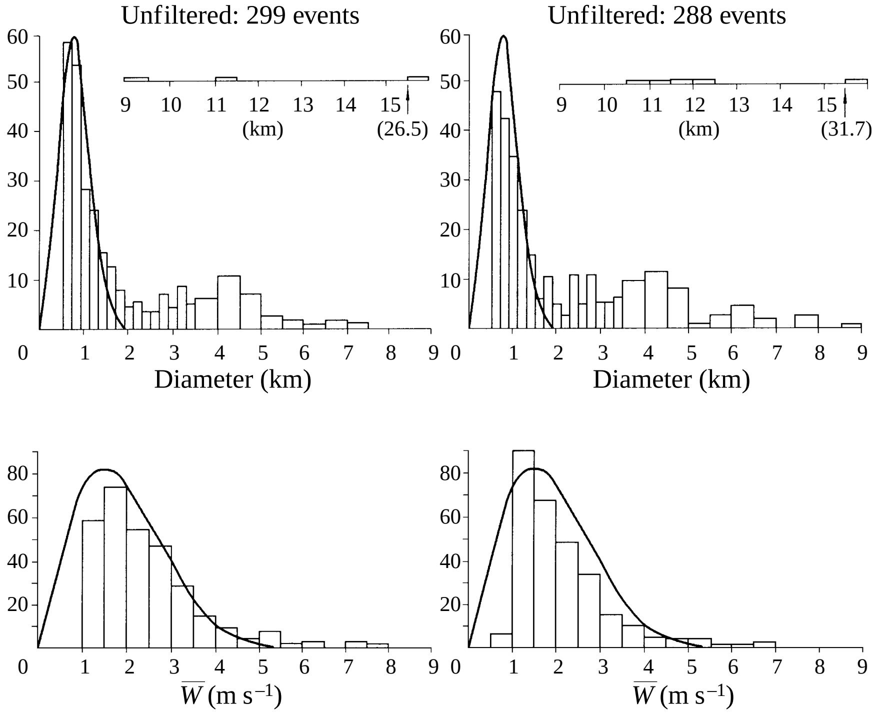

FIGURE 8. Comparison of calculations with observation data: repeatability of cloud diameters d (the upper part of the figure); repeatability of $\bar{W}$ (the lower part of the figure). Bold lines, calculations using (B.1), (B.2); rectangles, measurements.

explained by the fact that the measurements include mesoscale structures, which are larger than convective clouds.

The distribution with $\bar{W}$, which is the average value of w for areas where $w > w_{min}$ is shown in the lower part of the figure. The theoretical curve has been calculated by the following relation:

$$S(\bar{W}) = 200\frac{\bar{W}}{w_1^2}\ \exp\left(-\frac{\bar{W}^2}{2w_1^2}\right), \tag{B 2}$$

$$w_{max} = (\alpha\lambda)^{1/2}h, \quad \bar{W} = w_{max}/2, \quad w_1 = 2(\nu(\alpha\lambda)^{1/2})^{1/2} = 1.5 \text{ m s}^{-1}.$$

It is easily seen that agreement between the theory and measurements is better in the upper part of the figure than in the lower part of the figure. This is explained by the fact that updraughts in large mesoscale structures are usually much weaker than in convective clouds.

REFERENCES

ANDRE, J.-C. 1996 A Third-order-closure model for the evolution of a convective planetary boundary layer. In *Seminars on the Treatment of the Boundary Layer in Numerical Weather Predication, Reading, 6–10 September 1976,* pp. 205–233.

ANDREEV, V. & PANTCHEV, S. 1975 *Dynamics of Atmospheric Thermals.* Gidrometeoizdat, Leningrad (in Russian).

ARAKAWA, A. & SCHUBERT, W. H. 1974 Interaction of a cumulus cloud ensemble with the large-scale environment, part 1. *J. Atmos. Sci.* **31**, 674–701.

Bizova, H. L., Ivanov, V. N. & Garger, E. K. 1989 *Turbulence in the Atmospheric Surface Layer*. Gidrometeoizdat, Leningrad (in Russian).

Clever, R. M. & Busse, F. H. 1994 Steady and oscillatory bimodal convection. *J. Fluid Mech.* **271**, 103–118.

Davaile, A. & Jampart, C. 1993 Transient high-Rayleigh-number thermal convection with large viscosity variations *J. Fluid Mech.* **253**, 141–146.

Deardorff, J. W. 1974 Three-dimensional numerical study of turbulence in an entraining mixed layer. Boundary-Layer Met. **7**, 199–226.

Decker, W., Petch, W. & Weber, A. 1994 Spiral defect chaos in Rayleigh-Benard convection. *Phys. Rev. Lett.* **73**, 648–651.

Ebert, E. E., Shuman, U. & Stul, R. B. 1989 Nonlocal turbulent mixing in the convective boundary layer evaluated from large eddy simulation. *J. Atmos. Sci.* **46**, 2178–2207.

Etling, D. & Brown, R. A. 1993 Roll vortices in the planetary boundary layer. *Boundary Layer Met.* **65**, 215–248.

Glukhovskaya, T. V. & Ordanovitch, A. E. 1993 On turbulent convection in a plane horizontal layer *Izv. Ross. Akad. Nauk, Mekh. Zhidk. Gaza* **6**, 49–56.

Goldshtik, M. A. 1985 On the problem of turbulence. In *Stability and Turbulence*. Institute of Thermophysics, Siberian Division, Academy of Sciences of the USSR, Novosibirsk (in Russian).

Gutman, L. N. 1969 *Introduction to the Nonlinear Theory of Mesoscale Meteorological Processes*. Gidrometeoizdat, Leningrad (in Russian).

Jimenez, J., Wray, A. A., Saffman, P. G. & Rogallo, R. S. 1993 The structure of intense vorticity in isotropic turbulence. *J. Fluid Mech.* **255**, 65–90.

Kruger, S. K., McLean, G. T. & Qiang Fu 1995 Numerical simulation of the stratus-to-cumulus transition in the subtropical marine boundary layer. Part II: Boundary layer calculation. *J. Atmos. Sci.* **52**, 2852–2868.

Konovalov, D. A. 1970 On the problem of structure of thermals. *Proc. Chief Geophys. Observatory* pp. 123–128.

Kuo, H. L. 1965 On formation and intensification of tropical cyclones through latent heat release by cumulus convection. *J. Atmos. Sci.* **22**, 40–63.

Kuo, H. L. 1994 Further studies of the parameterization of the influence of cumulus convection on large-scale flow. *J. Atmos. Sci.* **31**, 1232–1240.

Kurbatskii, A. F. 1988 *Modeling of Non-local Turbulent Transport of Momentum and Heat*. Nauka, Novosibirsk (in Russian).

LeMone, M. A., Chang, T. C. & Lucas, C. 1994 On the effects of filtering on convective-core statistics. *J. Atmos. Sci.* **51**, 3344–3350

Ludlam, F. H. & Scorer, R. S. 1952 Bubble theory of penetrative convection. *Q. J. R. Met. Soc.* **79**, 1952.

Lykossov, V. 1995 Turbulence closure for the boundary layer with coherent structures: an overview. *Berichte aus dem Fachbereit Physik. Alfred - Wegener - Institut fur Polar - und Meeresforschung, September 1995, Rep.* 63.

Malbackov, V. M. 1972 On theory of thermals in stationary atmosphere. *Izv. Akad. Nauk SSSR, Fiz. Atm. i Okeana* **8**, 1972, 683–694.

Malbackov, V. M. 1978 On interaction of thermals. *Proc. West–Siberian Regional Research State Met. Institute,* pp. 75–85.

Malbackov, V. M. 1992 A simplified model of an ansemble of convective cells and construction of parameterization procedures for moist convection. *Izv. Akad. Nauk SSSR, Fiz. Atm. i Okeana* **28**, 901–914.

Malbackov, V. M. & Perov, V. L. 1993 Parameterization of convection in models of large-scale circulation of atmosphere. *Computational Processes and Systems*, No. 10 (ed. G. I. Marchuk), pp. 96–136 M.: Fizmatlit.

Malkus, J. S. & Veronis, G. 1958 Finite amplitude cellular convection. *J. Fluid Mech.* **4**, 225–235.

Mason, B. J. 1971 *The Physics of Clouds* Oxford, 2nd Edn.

Mazin, I. P. & Shmeter, S. M. 1983 *Clouds, Structure and Formation Physics*. Gidrometeoizdat, Leningrad (in Russian).

Mazin, N. P. & Ckrgian A. Ck. 1989 *A Cloud and Cloudy Atmosphere. Handbook*. Gidrometeoizdat (in Russian).

Mikhailova, L. A. & Ordanovitch, A. Ye. 1991 Coherent structures in the atmospheric boundary layer (a survey). *Izv. Atmos. i Okeanich. Fiz.* **27**, 413–428.

C.-H. Moeng, Lenshow, D. H. & Rendal, D. A. 1995 Numerical investigations of the roles of radiative and evaporative feedbacks in stratocumulus entrainment and breakup. *J. Atmos. Sci.* **52**, 2869–2883.

Noto, K., Yamamoto, Y. & Nakajima, T. 1994 Three-dimensional natural convection from a square plate with uniform surface heat flux. *Heat Transfer, 1994: Proc. 10th. Intl Heat Transfer Conf., Brighton,* pp. 531–536. Righby.

Rayleigh, Lord 1916 On convection current in a horizontal layer in fluid, when the higher temperature is on the under side. *Phil. Mag.* **32** 329.

Tiedtke, M. 1983 The sensitivity of the time-mean large-scale flow to cumulus convection in the ECMWF model. *Workshop on Convection in Large-Scale Numerical Models, ECMWF, 28, November - December 1983,* pp. 297–316.

Tiedtke, M. 1989 A comprehensive massflux scheme for cumulus parameterization in large-scale models. *Mon. Wea. Rev.* **177**, 1779–1800.

Vaskevitch, L. A. & Pushistov, P. Y. 1988*a* A comparative analysis of some statistical characteristics of vertical velocity and temperature deviation fields within thermals by numerical modeling and observational data. *Proc. West–Siberian Research hydrometeorological Institute, Novosibirsk* **85**, 84–91.

Vaskevitch, L. A. & Pushistov, P. Y. 1988*b* Frequency of occurrence and horizontal sizes of thermals in numerical simulations of an ensemble of penetrative convection in the atmospheric surface layer. *Proc. West–Siberian Research Hydrometeorological Institute, Novosibirsk* **85**, 91–97.

Veltichev, N. F. & Geokhlanian, T. H. 1974 Cell convection: Laboratory measurements and observations in the atmosphere. In *Proc. Hydrometeological center of the USSR*, No. 132, pp. 71–87.

Wilczak, J. M. & Businger, J. A. 1983 Thermally indirect motions in the convective atmospheric boundary layer *J. Atmos. Sci.* **40**, 343–358.

Wilkins, E. N., Sasaki, Y. & Marion, E. W. 1972 Laboratory simulation of wake effects on second and third thermals. *Mon. Wea. Rev.* **100**, 399–407.

Wolfson, A. I. 1961 *Investigation of Convective Motions in the Atmosphere.* Nauka, Moskwa (in Russian).